U.D.C. 539.121

Application of Mössbauer Spectroscopy in the Study of Surface Phenomena

V.I.Gol'danskii and I.P.Suzdalev

Recently there has been a considerable growth of interest in the elementary processes occurring on the surface of a solid or associated with the effect of the surface on the properties of atoms and molecules within the bulk of the solid. Mössbauer spectroscopy yields unique information about the electronic structure and the nature of the motion of atoms and therefore the use of this method is extremely effective in fundamental investigations of surface phenomena.
This review deals with the theoretical concepts of Mössbauer spectroscopy and the experimental data on its application in the physical chemistry of surface phenomena. A systematic account is given of new experimental results, which are compared with data obtained by other procedures.
The bibliography includes 70 references.

CONTENTS

I. Introduction 609
II. Phenomena on the surface of solids 609
III. Phenomena associated with the effect of the boundaries of the solid on the properties of internal atoms 620

I. INTRODUCTION

The development of the theory and technique of Mössbauer spectroscopy has revealed fields of research where its application is extremely effective. One such field, where the characteristics of the method give rise to a particularly large number of new possibilities, concerns surface phenomena[1,2]. During the several years of the application of the Mössbauer effect in the study of surface phenomena, many interesting and important results have been obtained in studies on the dynamics of the motion of atoms on the surface, their electronic state, the elementary steps in adsorption and catalysis, and also the physics of the highly dispersed state of matter.

Bearing in mind the differences between the types of surface effects, the surface phenomena investigated with the aid of Mössbauer spectroscopy may be conventionally divided into two classes. The first class is associated with the study of the state of atoms present directly on the surface of the solid. Here one investigates (1) the atomic vibrations on the surface, (2) surface diffusion, (3) the electronic states of atoms on the surface, (4) the magnetic properties of atoms on the surface, (5) the elementary steps in adsorption and the chemistry of surface compounds, and (6) catalysis.

The second class of phenomena is associated with the effects of the boundaries of the solid on the properties of its internal atoms. These include, for example, (1) the change in the phonon spectrum and the type of atomic vibrations in highly dispersed particles, (2) the variation of the magnetic properties of the particles (the phenomenon of superparamagnetism), and (3) topochemical reactions.

The study of all these processes involves a definite characteristic associated with the method, consisting in the fact that, in order to ensure a sufficiently large number of resonating nuclei on the surface of the solid (it is necessary to have at least 10^{17} nuclei per cm^2 when the probability of the Mössbauer effect $f' \simeq 0 - 0.3$), it is necessary to choose systems with high surface areas, amounting to hundreds of square metres per gramme. The surface density of atoms in a monomolecular layer is about 10^{15} nuclei per cm^2. However, it is possible to observe the effect for surface densities smaller by a factor of tens and hundreds (10^{13}–10^{14} nuclei per cm^2) if one uses as the test object a surface source of resonance γ-radiation, for example by depositing cobalt-57 nuclei on the test surfaces. Then the measurement of the spectra with the required statistical accuracy is determined solely by the duration of the experiment. Experiments where the test substance is employed as an absorber are simpler to perform and are more widely carried out. However, in many cases, for example in the study of the properties of atoms located on crystal boundaries, it is necessary to deposit radioactive nuclei on the surface investigated.

The necessity for the presence on the surface of a sufficiently large number of resonating nuclei in order that the Mössbauer effect may be observed naturally imposes limitations on the application of Mössbauer spectroscopy, particularly in the study of adsorption and catalysis at low surface coverages and also in the study of the surface of single crystals.

The characteristics of the results in the fields enumerated above are dealt with below.

II. PHENOMENA ON THE SURFACE OF SOLIDS

1. Atomic Vibrations on the Surface

The first theoretical calculations of Rich[3] and Maradudin[4] showed that the type of vibrations of atoms on the surface differs from that in the bulk of the solid. It was to be expected that the average of the square of the displacement of the atoms on the surface $\langle r^2 \rangle$ will be higher compared with the internal atoms and that the difference should increase with temperature. According to Rich[3], in a model comprising a cubic lattice extending to infinity at one end and in which account is taken only of the nearest neighbours, the probability of the Mössbauer effect at 90°K for the internal atoms is higher by 26% and at 284°K by 60% than for the surface atoms. Maradudin[4] drew attention to the fact that the vibrations of surface atoms are anisotropic. Thus, for the model with a cubic lattice of a central type taking into account the interactions with the nearest neighbours and the neighbours following

immediately beyond them, the average of the square of displacement in a direction perpendicular to the surface exceeds by a factor of two the corresponding values for the internal atoms, while along the surface $< x^2 >$ is greater by 30% than $< x^2 >$ for internal atoms. Calculations showed that the effect of the surface extends only over five layers. Kothari [5] found by calculating the ratio of the Debye temperatures for the surface and internal layers of the cubic lattice ($\theta_{eff}/\theta_0 \simeq 0.7$) that $< r^2 >_s$ for surface atoms exceeds by a factor of two $< r^2 >_i$ for internal atoms and is almost independent of the model. Analogous results were obtained by Corciovei [6]. Clark et al.[7] calculated $< r^2 >$ as a function of the distance from the free surface of the single crystal for a face-centred cubic lattice of nickel at a high temperature. The calculations were made for (100), (110), and (111) surfaces using a model of the central type taking into account the interactions with nearest neighbours in a crystal having a thickness of 20 layers. It was established that $< r^2 >$ increases monotonically from the centre of the crystal to its edges.

Burton and Godwin [8] and also Suzdalev [9] noted that the nature of the anisotropy of the atomic vibrations depends significantly on whether the atoms form part of the surface layer itself, i.e. on whether they are located within the surface or whether they are distributed on top of the surface under investigation (Fig. 1).

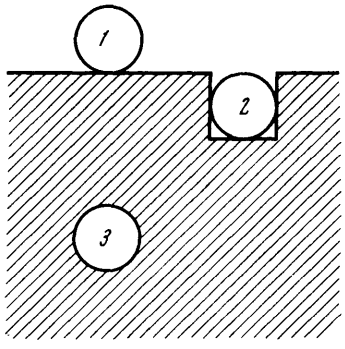


Figure 1. Atoms *on* the surface of the solid (*1*), *within* the surface (*2*), and within the solid (*3*).

Subsequently we shall use the following terminology: unless it is specified where the atoms are located, the term atoms *in* the surface will imply atoms within the surface when they are located in the interior of the surface layer and the term atoms *on* the surface will imply atoms distributed on top of the surface layer. The values of $< x^2 >$ and $< z^2 >$ on the surface have been estimated with the aid of a very simple model developed by Clark et al.[7] (Fig. 2) in which the force constants are proportional to the number of bonds between a given atom and the nearest neighbours and the next nearest neighbours (all the bonds are assumed to be of equal length and the bonds directed at right angles to the direction of the γ-radiation are disregarded). Fig. 2 presents three cases of bond location: *a* and *b*—atoms on the surface of the solid; *c* and *d*—atoms in the surface; *e*—atoms within the solid. The arrows indicate two different directions of γ-radiation.

Under these conditions the force constants κ are as follows:

(*a*) $\kappa \propto 1 + 4 = 5$ bonds
(*b*) $\kappa \propto 0 + 2 = 0$ bonds
(*c*) $\kappa \propto 1 + 4 = 5$ bonds
(*d*) $\kappa \propto 2 + 6 = 8$ bonds
(*e*) $\kappa \propto 2 + 8 = 10$ bonds.

Apart from showing a general increase of $< r^2 >$ on the surface, the model permits the estimation of the anisotropic vibration of the surface atoms. For atoms *within* the surface (*c* and *d*), the amplitude of the atomic vibrations at right angles to the surface is higher than along the surface:

$$\frac{\langle z^2 \rangle}{\langle x^2 \rangle} = \frac{8}{5} = \frac{\varkappa_x}{\varkappa_z}.$$

On the other hand, for atoms over the surface of the solid (*a* and *b*), the amplitude of the atomic vibrations along the surface is higher than at right angles to the surface:

$$\frac{\langle z^2 \rangle}{\langle x^2 \rangle} = \frac{2}{5} = \frac{\varkappa_x}{\varkappa_z}.$$

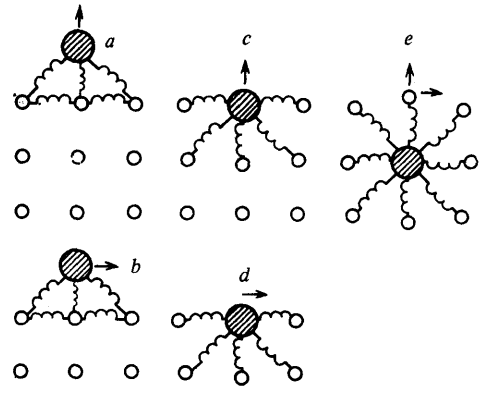


Figure 2. A model diagram illustrating the location of the atoms *on* the surface (*a*, *b*), *within* the surface (*c*, *d*), and within the solid (*e*) taking into account the interactions with nearest and next nearest neighbours.

Wallis [10] analysed the problem of the mean square velocities $< v^2 >$ of atoms on the surface of a solid and showed that on the surface these velocities are reduced, which leads to a decrease of the temperature shift of the Mössbauer spectral lines: $\delta E_D = E_\gamma < v^2 > /c^2$, where E_γ is the energy of the resonance transition.

A number of experiments have been performed to investigate the nature of the atomic vibrations on different surfaces. The type of vibrations of radioactive atoms in a planar surface of the usual kind was investigated by the surface emitter–bulk phase absorber method.

Allen [11] deposited 0.01 of a monolayer of cobalt-57 on the (100) and (111) silicon surfaces previously evacuated to 10^{-9} mmHg. The spectrum had two lines, which "merged" into one when the cobalt diffused into the silicon. For 300° and 800°K, the second-order Doppler effect resulted in a relative temperature shift $\delta E_D/E_D = 10^{-15}(-2.05 \pm 0.16)$ deg^{-1} for atoms on the surface and $\delta E_D/E_D = 10^{-15}(-2.17 \pm 0.16)$ deg^{-1} for internal atoms,

which confirms the decrease of $< v^2 >$ on the surface. On the other hand, analysis of the temperature variation of the probability of the Mössbauer effect $f(T)$ for cobalt-57 atoms on the surface of silicon and within the bulk of the crystal yielded the Debye temperatures $\theta_T = 555°K$ on the surface and $\theta_T = 588°K$ within the bulk of silicon.

Results contrary to the calculations [5-9], i.e. a decrease of $< r^2 >$ on the surface relative to the bulk phase of the solid, were obtained by Bowles and Cranshaw [12], who deposited electrolytically radioactive tin on platinum. They observed an increase in the probability of the effect (a decrease of $< r^2 >$) for tin monolayers compared with individual, even very small particles. However, one should bear in mind that this type of effect might have been caused by the diffusion of tin into the bulk of platinum.

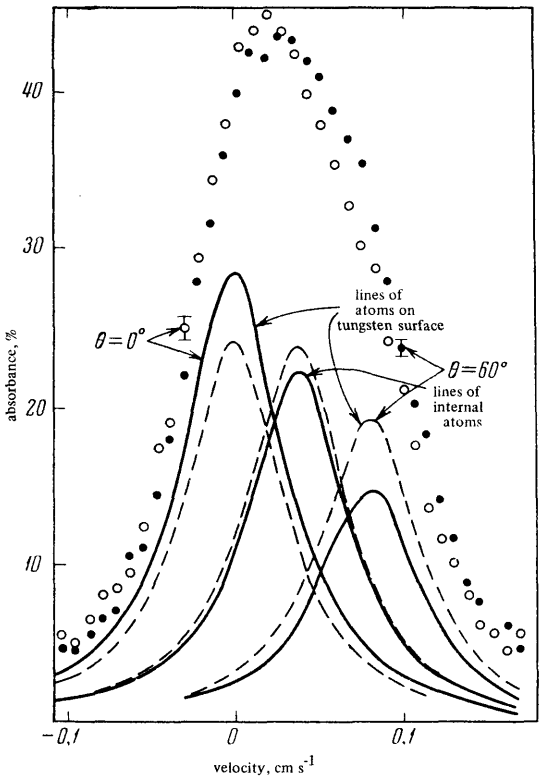


Figure 3. Spectrum of cobalt-57 on tungsten (300°K) with potassium hexacyanoferrate(II) as an absorber.

Burton and Godwin [8] investigated the cobalt-57 vibrations on single crystal and polycrystalline surfaces of tungsten and silver. Cobalt-57 was deposited on the metal by vacuum-evaporation (10^{-10} mmHg) in an amount corresponding to 0.1 of a monolayer (Fig. 3 shows the spectrum of cobalt-57 on tungsten). It is suggested that the spectrum consists of three lines—a doublet and a singlet—and that the asymmetric (due to the anisotropy of the thermal vibrations of cobalt-57 atoms) doublet is caused by cobalt-57 atoms on the surface of tungsten (as on silicon [11]), while the singlet corresponds to the cobalt which had diffused into the bulk of tungsten. Later it was found that $< r^2 >$ for atoms on the surface of tungsten increases relative to $< r^2 >$ for internal atoms and that the cobalt-57 vibrations on the surface are anisotropic:

$$\frac{\langle x^2\rangle_s}{\langle z^2\rangle_s} = 1.9 \pm 0.4 \text{ and } \frac{\langle x^2\rangle_s}{\langle z^2\rangle_i} = 2.5 \pm 0.5.$$

Since $< x^2 > > < z^2 >$, here the cobalt atoms are located on the tungsten surface and not *within* the surface. For cobalt-57 atoms on the surface of silver, it was found [8] that $< r^2 >_s < < r^2 >_i$. The result is contrary to the usual increase of $< r^2 >$ on the surface. It is also contrary to the measurements of the Debye temperatures of the surface and internal silver atoms by diffraction of slow electrons [13] with the electron energy varied from 40 to 240 eV. Jones et al. obtained a value for $< z^2 >$ on the surface of silver twice as high as for internal atoms. Therefore the results of Burton and Godwin [8] are probably associated with the formation on the surface of silver of highly dispersed cobalt-57 and the effect of its intrinsic properties and not that of the surface of silver.

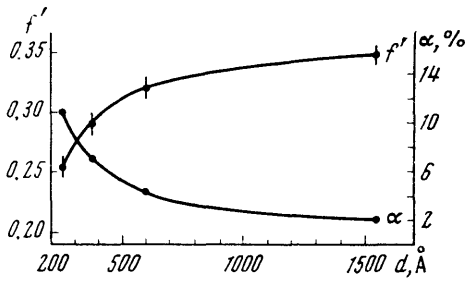


Figure 4. Variation with particle size of the probability of the Mössbauer effect f' and the specific surface α of particles of highly dispersed β-tin (77°K).

The use of large surface areas permits the study of atomic vibrations on the surface also with the aid of the bulk-phase emitter–surface absorber method. Thus the vibrations of atoms in tin dioxide on the surface of highly dispersed tin with a particle size of 300 Å were investigated [14] and a marked decrease of the probability of the Mössbauer effect compared with the probability for the usual tin dioxide was observed. The probability f' approached the normal value when the particles were fully oxidised. In another experiment [15] a study was made of the variation of f' and correspondingly of $< r^2 >$ for non-oxidised β-tin particles with $d = 250$ and 370 Å and $d = 650$ and 1550 Å. A decrease of f' with decrease of particle size was observed. Fig. 4 presents the function $f' = f'(d)$ and the variation of the specific surface $\alpha = f(d)$. The Debye temperature θ_D decreases from 140°K for $d = 1550$ and massive specimens to 120°K for $d = 250$ Å. For five surface layers, estimates yield $\theta_D = 100°K$. A decrease of f' was also observed for small tungsten particles by Roth and Hörl [16], although it was much smaller than might have been expected: $f' = 0.57$ for particles with a diameter of 30 Å and $f' = 0.61$ for particles with a diameter of 1 μm.

Van-Wieringen [17] noted that the vibrations of surface atoms are influenced by the matrix in which the dispersed particles are distributed. Thus, depending on the matrix,

f' ranging from 0.43 after incorporation in a matrix to 0.31 after preparation of a suspension in acetone and compression between two plates was obtained for Fe_2O_3 with a particle size of 30 Å.

In experiments with particles dispersed to an even greater extent, the nature of the vibrations of atoms on the surface is of course obscured by the vibrations of atoms within the particles.

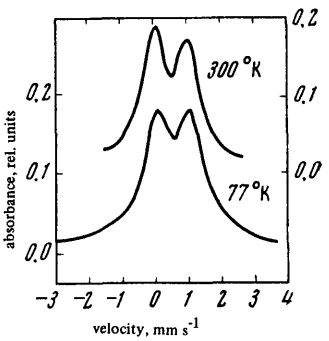


Figure 5. Spectrum of iron on the surface of η-Al_2O_3 at different temperatures.

A number of studies on the dynamics of the motion of surface atoms have been made under conditions where the Mössbauer atoms were sorbed on a large surface area. Such investigations were begun by Flinn et al.[18] with iron atoms on the surface of η-alumina and were followed by the present authors' experiments with tin on the surface of silica gel[19].

Spectra of iron, which is probably present in the form of Fe_2O_3 on the surface of alumina, are presented in Fig. 5. A striking feature is the asymmetry of the quadrupolar spectrum of Fe^{3+} on alumina, which is particularly pronounced at 300°K: $A = 0.94 = I_{3/2}/I_{1/2}$, where A is the ratio of the intensity of the doublet lines. This asymmetry, as well as the asymmetry observed in the study by Burton and Godwin[8] already noted above, is due to the anisotropy of the atomic vibrations on the surface. Assuming that the asymmetry of the components of the quadrupolar splitting is caused by the anisotropy of the probability of the Mössbauer effect (the Gol'danskii–Karyagin effect), Suzdalev et al.[18] found that $\langle z^2 \rangle - \langle x^2 \rangle = 10^{-18}$ cm^2. It was suggested that the electric field gradient is positive, i.e. the iron atoms are incorporated in the surface layer of the alumina lattice ($\langle z^2 \rangle > \langle x^2 \rangle$), in contrast to cobalt-57 on the surface of tungsten[8]. Generally speaking, in order to determine the sign of the electric field gradient, it is necessary to employ a single-crystal surface. Then, knowing the angle between the crystal field gradient (perpendicular to the surface) and the direction of the γ-beam, it is possible to determine unambiguously the sign of the crystal field gradient from the quadrupolar spectrum and hence the nature of the asymmetric vibrations.

The quadrupolar spectrum observed in studies[19,20] on tin (in the form of SnO) on the surface of a zeolite or silica gel with a pore diameter of 120 Å was also found to be asymmetric (Fig. 6). The asymmetry increased with temperature. Since in these experiments absolute values of f' were obtained, it proved possible to determine not only the difference $\langle z^{-2} \rangle - \langle x^2 \rangle$ but also each component separately: $\langle x^2 \rangle = 0.46 \times 10^{-18}$ cm^2 and $\langle z^2 \rangle = 1.76 \times 10^{-18}$ cm^2 at 210°K. Thus tin atoms are located within the surface layer of silica gel and the mean square of the displacement in a direction perpendicular to the surface of the globule exceeds by a factor of four the mean square of the displacement along the surface of the globule.

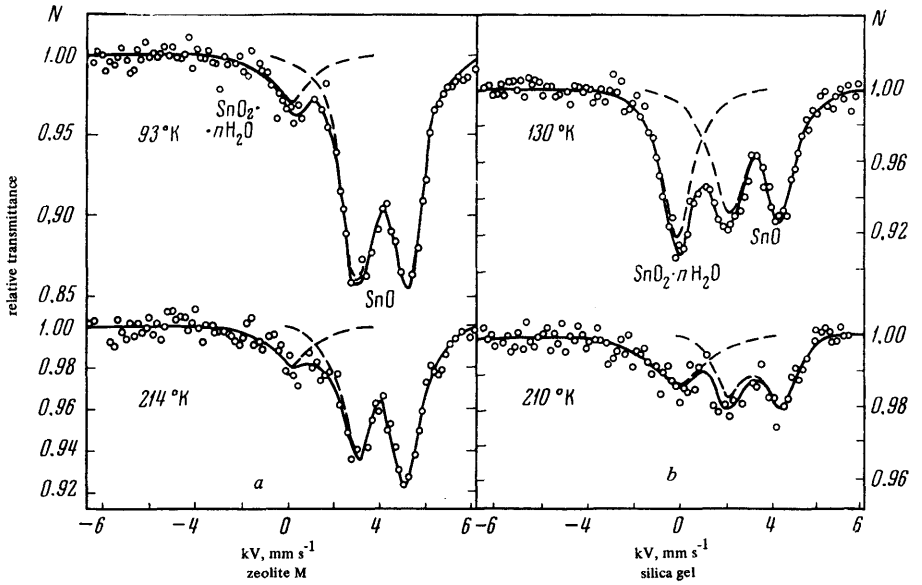


Figure 6. Spectrum of tin on the surface of a type M zeolite (mordenite) (*a*) and coarsely porous silica gel (*b*) at different temperatures. The left-hand line corresponds to $SnO_2.nH_2O$ and the two right-hand lines to SnO.

The temperature variation of the anisotropy of the atomic vibrations on the surface has been investigated theoretically and experimentally[20]. Silica gel and a zeolite with tin atoms on the surface were studied. When the Sn^{2+} ion on the surface was treated as a harmonic oscillator, a relation $A = f(T, \gamma)$ (γ is a parameter associated with the difference between the squares of the vibration frequencies of tin atoms in two directions at right angles) suitable for calculations was obtained:

$$A(T) = \frac{\int_0^1 (1+u^2)\exp(-\gamma T u^2)\,du}{\int_0^1 (5/3-u^2)\exp(-\gamma T u^2)\,du} \quad (u^2 = \cos^2\theta); \quad \gamma = \frac{\varkappa^2 k}{M}\left(\frac{1}{\omega_1^2}-\frac{1}{\omega_2^2}\right), \quad u^2 = \cos^2\theta$$

where κ is the wave number, M the mass of the particle, and θ the angle between the normal to the surface and the direction of the γ-ray beam. Fig. 7 presents the calculated values of $A = f(T)$ for different γ and shows satisfactory agreement between the experimental points and the calculated curve corresponding to $\gamma = 0.0045$ and $1/\omega_1^2$ and $1/\omega_2^2 = 4.5 \times 10^{-27}$ s^{-2}. This shows that the Sn^{2+} ion vibrates "along" the surface as a harmonic oscillator weakly interacting with its neighbours.

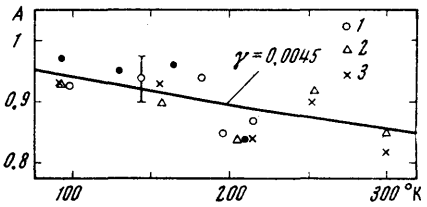


Figure 7. Temperature variation of the asymmetry of the quadrupole splitting lines of SnO on the surface of coarsely porous silica gels (*1*), a silica gel with fine pores (*2*), and a zeolite (*3*).

An important problem is also the elucidation of the effect of pore dimensions on the type of atomic vibrations, i.e. whether there are differences within the type of atomic vibrations on a surface close to the usual planar type and on a surface with an appreciable curvature. The vibrations of tin atoms on the surface of coarsely porous silica gel with pore dimensions of 120 and 250 Å, which is almost planar a relation to the tin atom and in silica gels with fine pores and a zeolite with nearly molecular pore dimensions were compared in the present authors' investigation[20].

Experiments on the temperature variation of the asymmetry of the vibrations showed that this kind of difference in pore dimensions does not affect the nature of the anisotropy of the vibrations but does influence the absolute values of $< r^2 >$. Probably $< r^2 >$ increases uniformly in all directions in the coarsely porous silica gels. In systems with pores having molecular radii, smaller values of $< r^2 >$ were observed for tin atoms on the surface than in coarsely porous systems, particularly at high temperatures.

However, the principal differences between the coarsely porous specimens and those having fine pores are shown in the diffusion pattern of tin atoms along the surface.

In conclusion and summarising the results obtained in this section, we may note that all the theoretical calculations associated with the increase of $< r^2 >$ and the anisotropy of the vibrations of atoms on the surface are largely consistent with the experimental data. An exception is the decrease of $< r^2 >$ and the corresponding increase of the probability of the Mössbauer effect for tin atoms on the surface of platinum[12] and for cobalt atoms on the surface of silver[8] (see in addition the remarks on pp. 610–611). We shall return to the discussion of this anomaly in the section dealing with the effect of the surface on the phonon spectrum of small particles.

2. Surface Diffusion

The diffusion of Mössbauer atoms may lead to an appreciable broadening of the observed lines in the γ-resonance spectra compared with their natural width. In solids the diffusion coefficients of atoms do not exceed 10^{-12} cm^2 s^{-1}, which gives rise to a widening significantly smaller than the natural line width. At the same time in liquids the diffusion coefficient is of the order of 10^{-5} cm^2 s^{-1} and therefore the experimental width exceeds by many powers of ten the natural width. However, in liquids there is no Mössbauer effect and therefore the widening of the experimental line cannot be observed. On the surface cases probably occur where the diffusion coefficients are in the intermediate range and therefore diffusion has a marked effect on line width in the Mössbauer spectra. The most probable mechanism of surface diffusion involves abrupt transition of atoms from one position to another. Then the widening of the line is determined by the Singwi–Sjolonder formula[21]: $\Delta\Gamma = 2h/\tau$ (h is the Planck constant, $\tau = l^2/6D_1$ the localisation time, l the distance between the localisation centres, and D_1 the coefficient of diffusion by "jumps"). For example in the case of iron τ must be less than 10^{-7} s^{-1} (for $l = 3 \times 10^{-8}$ cm) and D_1 must be greater than 10^{-9} cm^2 s^{-1} for appreciable widening to be observed. There exists yet another mechanism which operates, for example, in polymolecular adsorption, mainly continuous diffusion which leads to a widening

$$\Delta\Gamma = \frac{2E_\gamma^2 D_2}{\hbar c^2},$$

where E_γ is energy of the nuclear order of magnitude and D_2 the coefficient of continuous diffusion. The widening of the Mössbauer line is more sensitive to this type of diffusion; here it is sufficient for D_2 to exceed 10^{-11} cm^2 s^{-1}.

In a number of studies the surface diffusion of tin and iron atoms on the surfaces of silica gel[19,20], zeolites[22], and ion-exchange resins[23] was investigated. Tin was physically sorbed on the surface of silica gels and zeolites in the form of $SnO_2.nH_2O$. The temperature variation of line half-width was investigated. It was shown that in coarsely porous silica gels there is a phase transition in the adsorption layer at 200°K involving "jumps" by $SnO_2.nH_2O$ groups from one localised position to another, which leads to a marked line widening and a decrease of the probability of the Mössbauer effect. In silica gels with fine pores and in zeolites a phenomenon of this kind was not observed (with the exception of a slight widening at a higher temperature) probably because of the stronger bonds formed by $SnO_2.nH_2O$ with the surface in pores of molecular dimensions (Fig. 8). It was of interest to estimate the activation energy for the diffusion of the $SnO_2.nH_2O$ groups. Using the expression $\tau = \tau_0 \exp(Q/RT)$, the activation energies were found to be $Q \simeq 3.5$ kcal mole^{-1} for coarsely

porous silica gel and 7.5 kcal mole^{-1} for silica gels with fine pores[19]. A study was also made of the diffusion of Fe^{2+} ions in the pores of zeolites of type Y and M and in KU-2 ion-exchange resin[22-24]. An increase of temperature resulted in a widening of the Fe^{2+} line, which led to the estimates $\tau = 3.9 \times 10^{-8}$ s and $D = 0.7 \times 10^{-8}$ cm^2 s^{-1} at 213°K and $\tau = 2.2 \times 10^{-8}$ s and $D = 10^{-8}$ cm^2 s^{-1} at 300°K for the diffusion of Fe^{2+} in the channels of zeolite M (mordenite) in the presence of n-hexane molecules. The numerical values of τ and D are consistent with the data of Barrer et al.[25]

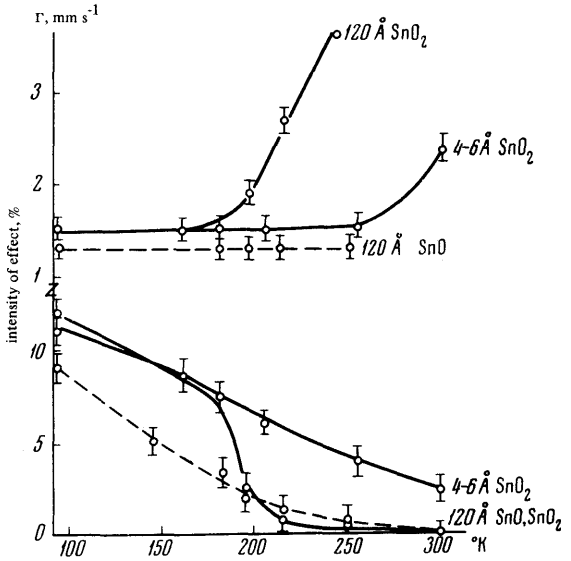


Figure 8. Temperature variation of the effect (%) and line width (Γ, mm s^{-1}) for tin on the surface of silica gels with pore diameters of 120 and 4–6 Å.

The diffusion of Fe^{2+} cations in the ion-exchange resin with sorbed hexane and water was investigated in greater detail (Fig. 9). The activation energy for diffusion in hexane was found to be 5 kcal mole^{-1} and for diffusion in water only about 1 kcal mole^{-1}, the diffusion of hexane occurring after its fusion (190°K). The lower activation energy for the diffusion of Fe^{2+} in KU-2 resin when water is present in the pores is probably due to the polarity of water molecules, which weakens the bond between the iron(II) cation and the resin lattice.

3. Electronic State of Atoms on the Surface

In this section we shall consider the problems of the type of electronic bonds involving the atoms on the surface compared with the bonds for atoms within the solid. It is difficult to expect that the valence of atoms will change on transfer to the surface. However, one may expect changes in the ionic character of the bond or in the mutual screening of the s, p, and d electrons. This might lead to a change of the isomer shift in the Mössbauer spectra of surface atoms. Such changes have not, however, been observed so far. Zeolites, where the pore dimensions are nearly molecular, appear to be an exception. Thus the isomer shift δE_I for Sn^{2+} in the type M zeolite[20] relative to SnO_2 increased from 2.7 mm s^{-1} (a value characteristic of the usual polycrystalline SnO) to 3.2 mm s^{-1} [henceforth the isomer shifts (IS) for tin will be reckoned relative to IS for tin dioxide and for iron relative to IS for sodium nitroprusside]. The above increase in isomer shift may be attributed, according to Donaldson and Senior[26], to a decrease of the contribution of the crystal field, which is very powerful in the normal compound SnO and leads to the mixing of the s and p electronic orbitals, thereby diminishing the isomer shift [i.e. the signal $|\Psi(0)|^2$]. Moreover, the atoms on the surface should be subject to the crystal field of lower symmetry compared with atoms within the bulk of the solid. This must lead to high electric field gradients the direction of which may be reasonably assumed to be perpendicular to the surface.

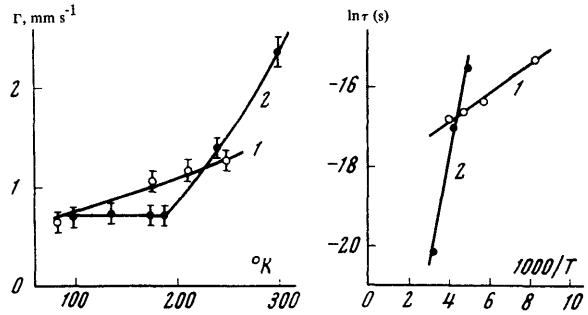


Figure 9. Increase in line width Γ for Fe^{3+} in an ion-exchange resin with increasing rate of diffusion of iron and the variation of the logarithm of the ion localisation time ($\ln \tau$) with temperature: *1*) water; *2*) n-hexane.

This may result in an increased quadrupole splitting in the Mössbauer spectra in the vicinity of the surface. Indeed in all the experiments the quadrupole splitting (QS) for surface atoms ΔE_Q increased and sometimes appeared even when the atoms within the bulk of the solid gave rise to no splitting at all. Thus Burton and Godwin[8] obtained $\Delta E_Q = 0$ for cobalt-57 atoms within a tungsten support and $\Delta E_Q = 0.78$ mm s^{-1} for cobalt-57 atoms on the surface of tungsten. For iron on the surface of η-alumina in the form of Fe_2O_3, Flinn et al.[18] observed an increase of QS from 0.3 mm s^{-1}, characteristic of the normal state of Fe_2O_3, to 1.06 mm s^{-1}. A similar increase of QS in consequence of the more important role of the surface was observed by Rumbic et al.[27] for highly dispersed Fe_2O_3 particles with dimensions of about 100 Å. Fig. 10 shows an increase of ΔE_Q as the particle size diminishes. Similar calibrations may be employed to estimate the particle size. An increase of QS for SnO on the surface to 2.1 mm s^{-1} compared with the normal value $\Delta E_Q = 1.3$ mm s^{-1} has been observed[19,20]. Finally the most striking feature is the occurrence of quadrupole splitting (ΔE_Q = 0.6 mm s^{-1}) in the Mössbauer spectrum of a metallic iron film 4.6 Å thick[28].

Continuing the discussion of the electronic state of atoms on the surface, we shall now deal with the magnetic properties.

4. Magnetic Properties of Atoms on the Surface

According to classical concepts, ferromagnetism is essentially a three-dimensional effect associated with the finite volume of matter[29]. Therefore magnetic ordering should not be expected for surface atoms. It is now known, however, that a hyperfine structure in Mössbauer spectra may arise not only in magnetically ordered systems but also in paramagnetic materials, provided that the relaxation time of electron spin is comparable to the precession time of the nuclear spin of the resonating atom[30,31]. Both spin–spin and spin–lattice relaxation is involved. At low concentrations of paramagnetic ions it is possible to ensure that the relaxation is wholly of the spin–lattice type. Since the paramagnetic ion on the surface is linked to the lattice less strongly than within the bulk of the solid, an increase in the spin–lattice relaxation time may be expected for surface atoms together with the appearance of a hyperfine structure in the Mössbauer spectra for such atoms, while those in the bulk phase do not give rise to a hyperfine structure.

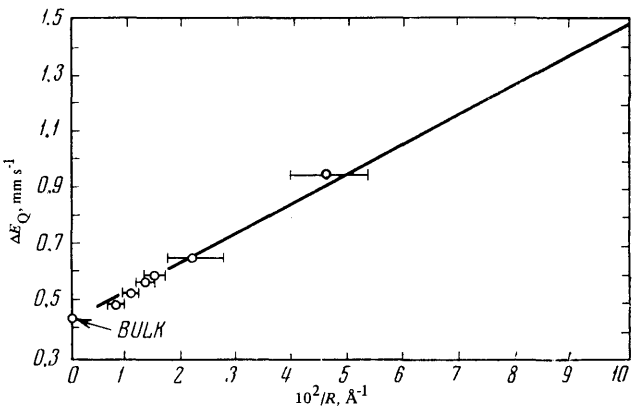


Figure 10. Variation of ΔE_Q with the reciprocal of the radius of highly dispersed Fe_2O_3.

The first result of this kind was obtained in the study of the relaxation of electron spin in ion-exchange resins[32]. The concentration of iron was extremely low (1.6 wt.%). A sharp increase in spin–lattice relaxation time was observed after the adsorption of water by this type of system. Fig. 11 presents the spectra of Fe^{3+} in a sulphonated ion-exchange resin before and after the adsorption of water. Water weakens the bond between Fe^{3+} and the resin lattice and increases the spin–lattice relaxation time τ. It was also noted that the increase of τ is accompanied by a decrease of the electric field gradient whenever it is caused by the withdrawal of the ion from the resin lattice and an increase in the symmetry in charge distribution occurring when the Fe^{3+} ion is surrounded by water molecules. We may note that, although the bond between the surface ion and the lattice is weakened, which leads to an increase of τ, the presence of high gradients may lower it (for two-phonon processes, which are responsible for relaxation in the case under discussion[32], the probability of spin–lattice relaxation is proportional to the square of the distance between the Stark levels, i.e. as a result of the increase of the electric field gradient and of the distance between the Stark doublets, the probability of relaxation increases and the relaxation time falls). Therefore Fe^{3+} ions in an ion-exchange resin exist under conditions more favourable for high relaxation times than in the case where Fe^{3+} is located on the usual type of surface, because the bond with the lattice is weak as on a normal surface but the electric field gradient is much weaker.

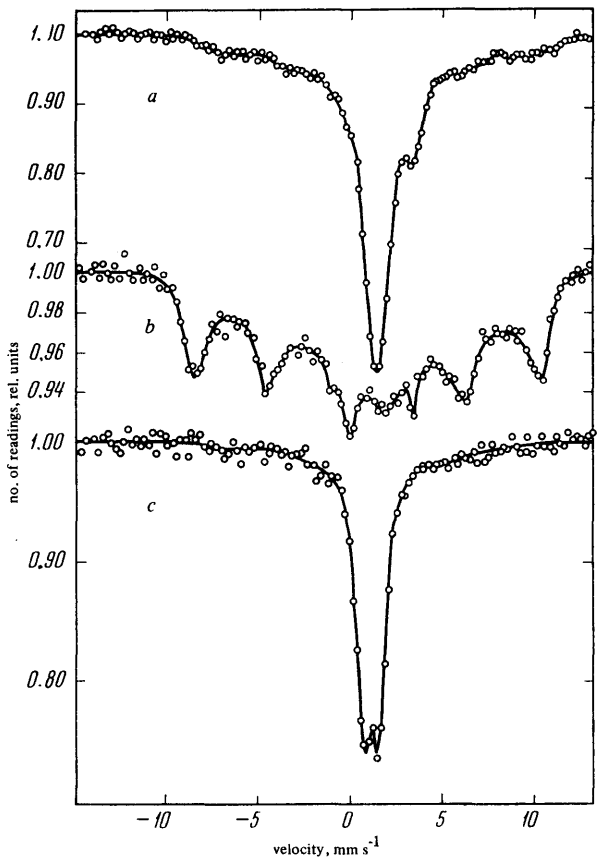


Figure 11. Spectra of a sulphonated resin with Fe^{3+} before (*a*) and after the adsorption of water (*b*) and of a phosphorylated resin after the adsorption of water (*c*) at 80°K.

Fig. 12 shows the temperature variation of the spin–lattice relaxation time for the Stark doublet $S_Z = \pm 5/2$ obtained experimentally and calculated using the Debye and Einstein approximations for $\theta_F = 325$°K and $\theta_D = 400$°K respectively[32]. θ_D determined in the usual way from the temperature variation of the probability of the Mössbauer effect is approximately the same. The vibration frequencies ($k\theta/\hbar$) of the lattice with Fe^{3+} obtained in this way are very high. Probably such high-frequency vibrations tend to average out the electric field at the Fe^{3+} ions and thereby retard the relaxation.

The effect of the immediate environment of the paramagnetic ion on the nature of spin–lattice relaxation has been investigated[33]. By sorbing different amounts of

water molecules in an ion-exchange resin, it has been shown that the hyperfine structure is fully formed and the maximum relaxation time $\tau = 2.4 \times 10^{-8}$ s is observed when there are six molecules of water for each iron ion. Then each spectrum corresponding to an intermediate average number of water molecules (n_{av}) per Fe^{3+} ion does not arise by a simple superposition of spectra with different values of n (for example the hyperfine structure due to four water molecules is not a result of the superposition of spectra with zero, 1, 2, 3, 4, 5, and 6 water molecules for each Fe^{3+} ion). This is evidence that the spectra of partly hydrated resin are observed. It was found that under certain conditions it is possible to observe the hyperfine structure due to Fe^{2+} in the ice lattice, for example in a strongly acid medium with an excess of chlorine atoms relative to iron (0.02 M $FeCl_3$ in 4.5 M hydrochloric acid). Since in the presence of between one and six water molecules per Fe^{2+} ion the ice lattice is not as yet observed in the ion-exchange resin (the distance between the ion-exchange centres is about 20–30 Å), one may conclude that the spin–lattice relaxation time is determined by the nearest environment of Fe^{3+}, i.e. the water molecules and not the entire ice lattice. Thus ion-exchange resins are very suitable for the investigation of the effect of various ligands on the relaxation of electron spin of the Fe^{2+} ion.

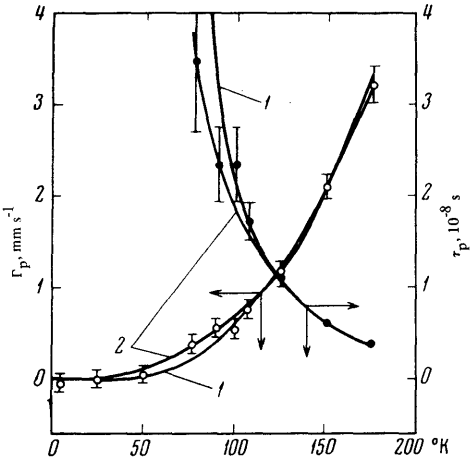


Figure 12. Temperature variation of the spin–lattice relaxation time of the Fe^{3+} ion and the width of the extreme spectral lines. The continuous curves were calculated using the Einstein (curve *1*) and Debye (curve *2*) approximations.

Widely occurring phenomena, such as adsorption and catalysis, are directly associated with the electronic and magnetic properties of atoms on the surface.

5. Elementary Steps in Adsorption. The Chemistry of Surface Compounds

The interaction of atoms or molecules with the surface of a solid leads, on the one hand, to a change in the state of the adsorbent atoms on the surface and, on the other hand, also in the properties of the sorbed groups themselves, i.e. the properties of the adsorbate. This entails a change in both the dynamic and electronic properties of atoms, which should be reflected in the Mössbauer spectra. The method employed in such experiments involves the use of an absorber of resonance γ-quanta as the adsorbate or the adsorbent. In order to obtain the Mössbauer spectra, it is necessary to have an adsorbent or adsorbate with atoms containing resonating nuclei and to follow the changes in the state of either the surface of the solid or of the sorbed substances. In some cases it is possible to follow both provided that the adsorbent and the adsorbate contain resonating nuclei. The application of Mössbauer spectroscopy makes it possible to distinguish physical sorption and chemisorption.

Since the bond between the surface atoms and the adsorbate is weaker in physical sorption than in chemisorption, the probability of the Mössbauer effect should be lower in physical sorption and the temperature variation more pronounced than in chemisorption, particularly at high temperatures. A distinction of this type was made[19] for $SnO_2.nH_2O$ physically sorbed on the surface of silica gel and Sn^{2+} chemisorbed as SnO. For physical sorption (Fig. 8), a more pronounced temperature variation of the probability of the effect was observed than in the case of chemisorption.

Moreover, since chemisorption entails a change in the electronic structure of both the adsorbent and the adsorbate, a radical rearrangement of the Mössbauer spectrum can be observed—with a change in the isomeric shift and quadrupole splitting, which is not a characteristic feature of physical sorption.

Physical sorption was investigated as a function of the number of monolayers of sorbed tin tetrachloride molecules on silica gel and a study was made of systems with pores whose size ranged from several hundred of angstroms to nearly molecular dimensions[20].

After the adsorption of $SnCl_4$ on silica gel, the form of the spectra hardly changed; the smallest decrease of the isomeric shift was observed in sorption on silica gel with nearly molecular pore dimensions.

A significantly different temperature variation of f' was observed on silica gels with fine pores for $SnCl_4$ sorbed in amounts less than one monolayer and in amounts corresponding to about five layers. The temperature variation of f' was much more pronounced for a large number of $SnCl_4$ layers than for a small amount, which is evidence that in physical sorption the $SnCl_4$ molecules are much more strongly bound to the surface of silica gel than to one another. For systems with fine pores, such a difference between the characteristics of the spectra with different numbers of sorbed layers is less marked.

The adsorption of water in ion-exchange resins was also investigated on the basis of changes in the probability of the Mössbauer effect[23]. The adsorption of water is known to lead to swelling of the resins and to a change in the state of the ion. KU-2 and KB-4 cation-exchange resins with the cations Fe^{3+} and Fe^{2+} and AV-16 and AV-17 anion-exchange resins with the anions $[Fe(CN)_6]^{3-}$ and $[Fe(CN)_6]^{4-}$ were investigated. All the ion-exchange resins were organic polymers or copolymers with functional groups capable of ion exchange. In KU-2 and KB-4 cation exchangers these are $R-SO_3^-$ and $R-COO^-$ groups respectively, in AV-16 anion exchangers these are the R_2NH, R_3N, and R_4N^+ groups, while AV-17 anion-exchange resins contain R_4N^+ groups. Whereas in KU-2 sulphonated resin the Mössbauer effect disappeared as a result of the adsorption of water, in KB-4 resin it per-

sisted after such adsorption. This result is associated with the dissociation of water molecules and Fe^{3+} ions from the lattice of KU-2 sulphonated resin. Analysis shows that[24] (Fig. 13) three water molecules for each Fe^{2+} ion are required for complete dissociation of the iron cation from the SO_3 group in the resin and the disappearance of the Mössbauer effect. It has also been shown that the Mössbauer effect does not decrease because part of the ions are dissociated while others are not. For small amounts of water (up to three molecules per ion), $< r^2 >$ increases and f' falls but Fe^{3+} ions remain localised (undissociated), while in the presence of a large amount of water Fe^{3+} ions cease to be localised, which leads to their diffusion by abrupt transitions ("jumps") from one localised position to another and the complete disappearance of the Mössbauer effect with simultaneous widening of the line due to diffusion. On the basis of the literature data[24,33] and the finding that the lines in the Mössbauer spectrum do not become wider when the average amount of water increases up to three molecules per Fe^{3+} ion while in the case of more pronounced hydration the lines do widen with increase of temperature owing to diffusion, one may conclude that the variance of the number of water molecules per metal ion is small.

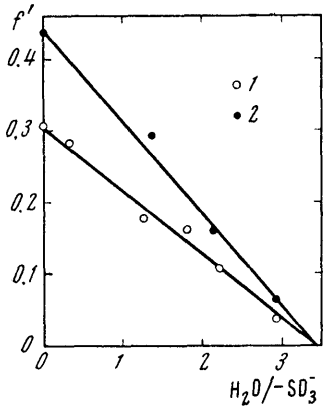


Figure 13. Decrease of the probability f for Fe^{3+} in a sulphonated ion-exchange resin after the adsorption of different numbers of water molecules per sulpho-group (300°K): *1*) resin with 12% of divinylbenzene as a cross-linking agent; *2*) non-swelling resin.

The effect of the degree of cross-linking of the sulphonated resin on the melting point of ice in the resin, at which the Mössbauer effect disappears, has been investigated[24]. It was found that an increase in the degree of cross-linking entails a shift of the point of disappearance of f' towards higher temperatures, probably due to the concentration of Fe^{3+} ions in the vicinity of the exchange centres. In the carboxylic acid KB-4 resin and in a phosphonic acid resin[32] there is probably an increase of $< r^2 >$ for Fe^{3+} ions and a decrease of f' but not complete dissociation of Fe^{3+} from the COO^- and CO_2^- groups.

Krizhanskii and coworkers[34] and Mackey and Collins[35] studied ion-exchange resins with the anions $[SnCl_6]^{2-}$ and iron cations respectively. Mackey and Collins found that in sulphonated cation exchangers there are two types of Fe^{3+} cations, with normal and anomalously high values of ΔE_Q ($\Delta E_Q = 1.6$ mm s^{-1}). They suggested that lines with high quadrupole splitting arise as a result of the hydrolysis of Fe^{3+} and the formation of hydrated dimers with an excess electron. However, one should bear in mind that the adsorption of water results in the appearance of a magnetic hyperfine structure in the spectrum[32], which covers a wider range of velocities than was examined by Mackey and Collins[35] and therefore the lines attributed to anomalous quadrupole splitting might have been simply part of a magnetic hyperfine structure, which had not been detected. Delgass and Boudart[36] observed a change in the probability of the Mössbauer effect in a type Y zeolite after the adsorption of water. Probably the decrease of f' is associated in this case with the increase of $< r^2 >$ for Fe^{3+} ions, as in ion-exchange resins[24], and not with the fact that part of the ions are dissociated and others are not, as suggested by Delgass and Boudart[36]. The adsorption of water can lead to an increase in the spin–lattice relaxation time too, as noted earlier[32,33] for Fe^{3+} in a sulphonated ion-exchange resin. An increase in spin–lattice relaxation time for Fe^{3+} ions was also observed after the adsorption of water, methanol, n-hexane, and tetramethyltin in zeolites of types Y and M containing Fe^{3+}, with a consequent asymmetry in quadrupole splitting of the Blume type[22,37], associated with the effect of electron spin relaxation on the Mössbauer spectra. Moreover, the adsorption of the substances enumerated above also led to the appearance of new lines in the spectrum, corresponding to divalent ions[22]. Since it is difficult to suppose that the adsorption of substances such as, for example, n-hexane leads to the reduction of iron in the zeolite, the appearance of the new lines may be attributed to the localisation in the zeolite channels of divalent iron ions which had been non-localised before adsorption and which had not given rise to a Mössbauer spectrum. The hypothesis of the presence of two types of cations in zeolites has been put forward previously by Dubinin[38] and Neimark[39]. The weak bond between Fe^{2+} and zeolite is characterised by the diffusion of the cation along the zeolite channel, which is reflected in a strong temperature-induced widening of the Fe^{2+} line.

All the previous experiments were related in one way or another to physical sorption, i.e. did not lead to a radical change in the spectrum. It is extremely interesting to investigate chemisorption by following the changes in Mössbauer spectra. When iron-containing zeolites were studied[22], the spectra of the $(CH_3)_4^{119}Sn$ adsorbate were also obtained and the presence of a bond between tetramethyltin molecules and $[AlO_4]^-$ was demonstrated. Similar spectra were obtained by Karasev et al.[40] in a study of the chemisorption of $(CH_3)_4Sn$ on alumina.

Morice and Rees[41] studied the adsorption of water and methanol on zeolites of types Y and M evacuated at 360°C. The adsorption of water or methanol resulted in a marked change in the spectra, the disappearance of certain forms of iron from the zeolite, and the appearance of others. It is at present difficult to identify all the forms of iron in the zeolites in experiments of this kind before and after adsorption.

The adsorption of polar solvents in zeolites alters the quadrupole splitting, the change being different for the Fe^{3+} and Fe^{2+} ions (see, for example, Refs. 22–24)—the quadrupole splitting increases for Fe^{2+} and decreases for Fe^{3+}. The results for Fe^{2+} probably indicate the formation of new chemical bonds, i.e. refer to chemisorption, while those for Fe^{3+} are related to water molecules surrounding the hydrated Fe^{3+} ion and diminishing the electric field gradient.

The experimental results for the chemisorption of iron(III) oxide on SiO_2 or Al_2O_3 carriers are easier to interpret. In this connection, we shall consider the studies of the oxidation and reduction of surface atoms. Hobson et al.[42,43] investigated the reduction of iron(III) oxide (Fe_2O_3) with different particle sizes on alumina and silica. The initial spectrum corresponds to highly dispersed Fe_2O_3 and reveals the very high value $\Delta E_Q = 1.87$ mm s^{-1}, which constitutes a record. Using the variation of the quadrupole splitting with particle size (Fig. 10) and extrapolating it to smaller particle sizes, Hobson and coworkers[42,43] estimated the dimensions of their own particles (about 20 Å). After the chemisorption of hydrogen, the spectra changed sharply. The authors postulate the presence of two forms of iron—the reduced, divalent iron with $\delta E_I = 1.35$ mm s^{-1} and $\Delta E_Q = 1.65$ mm s^{-1} corresponding to the usual ionic iron compounds and trivalent iron with $\delta E_I = 1.02$ mm s^{-1} and $\Delta E_Q = 0.98$ mm s^{-1}. For these particle sizes, reduction to metallic iron does not take place. The reduction of larger Fe_2O_3 particles on alumina[43] gave a mixture of metallic and divalent iron. The authors conclude that the smaller particles of silica gel cannot be reduced to metallic iron at all.

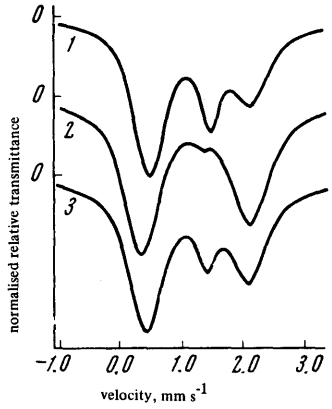


Figure 14. Spectra of iron on silica before (curve *1*) and after (curve *2*) chemisorption of ammonia.

Hobson studied the chemisorption of ammonia on iron(III) oxide obtained by preliminary heat treatment of silica gel impregnated with iron(III) nitrate[44]. Fig. 14 shows the spectra before chemisorption (curve *1*), after chemisorption (curve *2*), and after repeated degassing (curve *3*). The kinetic data indicate dissociative adsorption of ammonia in this system. Spectrum *3* shows the reduction of trivalent iron by ammonia, since the amine radical formed can supply electrons to the iron *d* orbital and thereby facilitate the formation of a high-spin iron(II) complex.

After the desorption of ammonia, the initial spectrum is restored[3]. These experiments characterise the change in the state of the adsorbents after chemisorption.

A series of experiments on the chemisorption of $(CH_3)_4Sn$ on silica gel and alumina were made by Karasev and coworkers[40,45], who showed that the form of the spectrum depends significantly on adsorption temperature. The spectra of freshly prepared specimens at 30°C differed sharply from those of specimens kept for 24 hours and longer in air. Fig. 15 shows the spectra of the initial $(CH_3)_4Sn$ adsorbed at 30°C on alumina and kept in air for 20 and 35 h. At an adsorption temperature of 30°C two additional peaks (curve *2*), which were attributed to the doublet of chemisorbed $(CH_3)_4Sn$, were observed in addition to the initial spectrum of tetramethyltin. The chemisorption centres are either oxygen or hydroxy-groups.

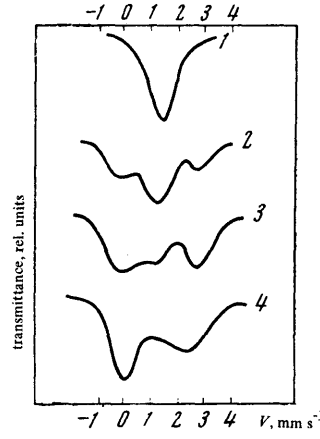


Figure 15. Spectra of $(CH_3)_4Sn$ chemisorbed on γ-Al_2O_3: *1*) initial spectrum of $(CH_3)_4Sn$ before chemisorption; *2*) after chemisorption; *3*) and *4*) after exposure to air.

The authors attribute the presence of the initial substance to physically sorbed $(CH_3)_4Sn$. When the specimen is kept for 20 h at room temperature (curve *3*), the intensity of the doublet increases. Further exposure to air leads to a radical alteration to the spectrum. Two lines appear, one of them (with $\delta E_I = 0$) is assigned to the chemisorption of $(CH_3)_4Sn$ involving the dissociation of tin–methyl bonds and the formation of a bond between the tin and oxygen atoms at the site of the aluminium vacancies; the second line is due to the bond between tin and aluminium and the surface dissociation of $(CH_3)_4Sn$. Chromatographic analysis of the gas phase over γ-alumina with adsorbed $(CH_3)_4Sn$ reveals the presence of ethane and methane, which may be attributed to the dissociative chemisorption of $(CH_3)_4Sn$.

To conclude this section, we emphasise yet again the principal results obtained in the study of the elementary adsorption steps. For physical sorption, these are (a) the observation of a more pronounced interaction of sorbed $SnCl_4$ molecules with the adsorbent than with one another; (b) the determination of the type of interaction between water molecules and iron cations in ion-exchange resins (the weakening of the bond between the cation and the lattice, dissociation in two stages, the presence of a definite number of water molecules per metal ion in the dissociation process, an increase in the spin–lattice relaxation time); (c) localisation of cations after the adsorption of molecules in the zeolite.

For chemisorption the following results were obtained: (a) the demonstration of the presence of two types of iron ions on the surface of silica gel after the chemisorption of hydrogen and the presence of a variety of forms of iron in zeolites; (b) demonstration of the adsorption of ammonia

with formation of an iron(II) complex; (c) the existence of two types of active centres for the chemisorption of tetramethyltin.

6. Heterogeneous Catalysis

Two aspects of the application of Mössbauer spectroscopy in this field must be distinguished: (1) the determination of the relation between the rate and selectivity of catalytic reactions on the one hand and the electronic state of the catalyst atoms on the other; (2) the observation of intermediate complexes in catalysis.

For the first aspect, it is sufficient to obtain the Mössbauer spectra of the catalysts before or after the catalytic reaction and to compare the parameters of these spectra with catalytic activity.

In order to investigate the second range of problems, it is necessary to have at one's disposal a Mössbauer proton spectrometer in which the reaction takes place directly in the zone where the spectra are recorded. Experiments of the second type have not as yet been achieved.

It is of considerable interest to investigate the relation between catalytic activity in any one reaction with parameters such as the isomeric shift and the quadrupole splitting in the Mössbauer spectrum. Probably catalytic activity should be related to both parameters and therefore in order to investigate correlations of this kind separately, it is necessary to have catalysts with variable catalytic activities and variable isomeric shifts for constant quadrupole splitting or conversely. It is simpler to vary the quadrupole splitting in a series of solid solutions for a constant isomeric shift.

The catalytic activities and selectivities of a number of iron- and tin-containing mixed oxide catalysts of the type of $X_aO_bM_cO_d$ solid solutions, where M is a Mössbauer atom and X a non-Mössbauer atom, have been compared[46]. For Fe^{3+} or Sn^{4+}, which have the symmetrical configurations $3d^5$ and $4d^{10}$, it is possible to alter the quadrupole splitting by varying X without changing the isomeric shift. The quadrupole splittings for these configurations are associated solely with the effect of the crystal field on these ions.

The oxidative ammonolysis of propene on catalysts of this kind has been investigated in this way. The reaction may take place via two pathways:

$$C_3H_6 + O_2 + NH_3 \begin{cases} \nearrow CH_2{=}CH{-}CN \\ \searrow CO_2 \end{cases} \quad \text{(acrylonitrile—AN).}$$

The curves relating the rate of formation of acrylonitrile to quadrupole splitting for a constant isomeric shift have a maximum. Similar "bell-shaped" curves are observed for the relation between the rate of reaction and the heat of formation Q of the surface compounds. An increase in the crystal field gradient and in the distortion of the lattice leads to an increase of Q and therefore at a certain value of the quadrupole splitting the rate of formation of acrylonitrile should be a maximum.

In order to investigate the possible mechanism of the catalysis, it is, however, necessary to choose simpler reactions involving one pathway only, such as for example, the classical catalytic oxidation of carbon monoxide to carbon dioxide on iron(III) oxide. An investigation of this kind was made[47] on a highly dispersed iron(III) oxide, the results of the Mössbauer experiment being compared with the kinetic data. In order to increase the fraction of surface ions, a highly dispersed iron(III) oxide with a particle size of about 80 Å and less was employed. The Mössbauer spectrum of such particles consisted of a paramagnetic component and a component with a magnetic hyperfine structure (Fig. 16). Several modifications of this experiment have been performed: (a) catalytic oxidation of carbon monoxide to carbon dioxide with and without freezing out the reaction product (carbon dioxide); (b) chemisorption of carbon monoxide on the specimen; (c) interaction of carbon monoxide with the specimen in the absence of oxygen with carbon dioxide frozen out; (d) heat treatment of the specimen with carbon monoxide and subsequent chemisorption of oxygen. The experiments were carried out at 100°C. The spectra and the kinetic measurements lead to definite conclusions concerning the mechanism of the catalytic oxidation of carbon monoxide to carbon dioxide, in agreement with Hauffe's data[48]. After the reaction of carbon monoxide with the catalyst surface, iron(II) cations bound firmly to the surface of Fe_2O_3 appear, the state of the iron remaining unchanged after heating to 100°C. The kinetic results show that there is a complete correspondence between the amount of carbon monoxide which has reacted with Fe_2O_3 and the amount of carbon dioxide frozen out.

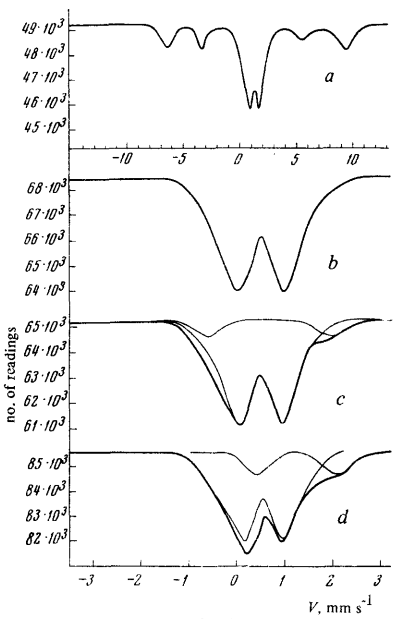


Figure 16. Spectra of iron(III) oxide in the catalytic oxidation of carbon monoxide to carbon dioxide: *a*) before oxidation; *b*) before oxidation at relatively low velocities of the source and absorber (the "paramagnetic" component of the spectrum is shown); *c*) after chemisorption of carbon dioxide; *d*) after chemisorption of carbon monoxide for measurements at room temperature.

This finding shows that the role of carbon monoxide involves in this case simply the reduction of Fe^{3+} to Fe^{2+} on the surface of the Fe_2O_3 particles without the formation of any surface compounds of carbon monoxide with iron(III) oxide. As a result, divalent iron ions appear on the surface of the particles and form a compound of the type of FeO. Indeed, the value $\delta E_I = 1.29 \pm 0.08$ mm s^{-1}, determined from the spectra, agrees with the value $\delta E = 1.32 \pm 0.06$ mm s^{-1} for the usual polycrystalline state of FeO.

However, the value $\Delta EQ = 1.67 \pm 0.08$ mm s^{-1}, obtained for the surface compound FeO, greatly exceeds $\Delta EQ = 0.77 \pm 0.03$ mm s^{-1} for the usual polycrystalline state of FeO. The observed increase of quadrupole splitting on the surface of iron(III) oxide may be attributed to the breakdown of symmetry in the distribution of atoms on the surface of the solid. The carbon monoxide molecules chemisorbed on the surface of Fe_2O_3 bind the oxygen of the catalyst and are desorbed in the form of CO_2 from the surface, leaving behind the Fe^{2+} ions. After the chemisorption of oxygen, the initial state of Fe_2O_3 is restored. A somewhat different process takes place after the adsorption of carbon monoxide on Fe_2O_3 (Fig. 16)—a surface compound with a fairly asymmetric configuration is formed. A similar surface compound arises when the catalytic oxidation of carbon monoxide is carried out without freezing out the carbon dioxide. When carbon dioxide is frozen out, the spectrum does not change. Probably the catalytic oxidation of carbon monoxide on Fe_2O_3 involves alternate reduction and oxidation of the catalyst. In the chemisorption of carbon monoxide the active part of the Fe_2O_3 surface is reduced to FeO, as a result of which carbon dioxide is formed. Oxygen in the gaseous mixture reoxidises FeO to Fe_2O_3.

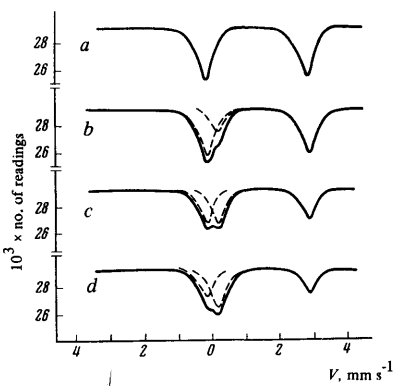


Figure 17. Spectra of Fe^{2+} on the surface of quartz before the pyrolysis of acetylene (*a*) and 0.5, 2, and 5 min (*c*, *b*, and *d*) after the start of the reaction (T_{exp} = 300°K).

In another study dealing with the pyrolysis of acetylene over an iron-containing quartz surface[49] an anomalous transparency of a film of pyrocarbon produced in the course of the reaction of acetylene with the iron atoms on the surface was observed. By evaporating Fe_2O_3 enriched with the iron-57 isotope to the extent of 91%, iron was deposited on the surface of quartz in the form of a divalent compound, probably iron(II) silicate ($FeSiO_3$) and also in the form of metallic iron and Fe_2O_3. After the pyrolysis of acetylene over this type of catalyst, there appears in the spectrum a line corresponding to a symmetrical surface compound, the amount of which increases with the duration of pyrolysis to a definite value, which is probably associated with the attainment of equilibrium between the complex formed in the reaction and the amount of iron(II) silicate present on the surface (Fig. 17). A layer of pyrocarbon with a thickness of several hundred angstroms, which is permeable in further penetration by acetylene to the quartz surface, is formed in the pyrolytic process on quartz. A control experiment was performed in which quartz with pyrocarbon on its surface was placed in a reactor with an argon atmosphere; under these conditions, iron was not bound in a surface complex, i.e. acetylene is essential for the formation of the complex. When the pyrocarbon was burnt off, the complex did not disappear either, which shows that the complex is located on the surface and is not bound to the bulk phase of the pyrocarbon. A similar conversion of metallic iron into the same complex has been observed.

In conclusion of the discussion of this class of phenomena, mention must be made of a new field in the chemistry of the solid state—the application of Mössbauer spectroscopy to surface phenomena, which permits the study of elementary processes on the surface taking into account the electronic and vibrational states of the atoms.

III. PHENOMENA ASSOCIATED WITH THE EFFECT OF THE BOUNDARIES OF THE SOLID ON THE PROPERTIES OF INTERNAL ATOMS

1. The Change in the Phonon Spectrum of a Substance in a Highly Dispersed State

In this section we shall consider the characteristic vibrations of atoms in small particles of a substance obtained by observing the changes in the probability of the Mössbauer effect. The changes in f for highly dispersed particles are associated with two effects: the first is the influence of the surface already mentioned above, which should lead to an increase of $\langle r^2 \rangle$. Since a decrease of particle size entails an increase in specific surface, f falls for this reason alone.

The second effect is associated with the change in the nature of the phonon spectrum itself for such particles and may act in the opposite sense, i.e. lead to an increase of f as the particle size is reduced. Marshall and Wilenzik[50], who assumed that for small particles the Debye approximation is applicable, concluded that the phonon spectrum must be displaced towards shorter wavelengths, which leads to an increase of f as the particle size is reduced. In fact, there is an upper limit to the wavelengths of phonons due to the dimensions of the particles themselves and therefore the phonon spectrum for small particles shows a more marked "cut off" on the long wavelength side (low frequency side) and, since the probability of the Mössbauer effect increases very markedly as the ratio $R/\hbar\omega$ falls (R is the recoil energy and ω the effective average vibration frequency), the low-frequency "cut off", which increases $\overline{\omega}$, results in a marked increase of f. Marshall and Wilenzik's reasoning is based, however, on the assumption that the Debye approximation is applicable to small particles. Actually, the phonon spectrum of small particles differs sharply from the usual spectrum by a set of discrete frequencies due to the presence of a finite number of atoms in such particles, which may lead to a change in $\overline{\omega}$ such that f will fall as the particle size is reduced. When account is taken of the decrease of the wavelength of the real phonon spectrum as a result of the effect of the surface, it is possible to predict the changes of f for particles of different kinds. The following in many ways contradictory results have been obtained experimentally. For β-tin particles, f falls with particle size (from 1550 to 250 Å)[15], while for gold particles it actually increases[50]. For small tungsten particles, f is also smaller than for foil[16].

For platinum[36], the probability of the effect hardly changes with particle size. Apart from these experiments, we investigated the changes in f for particles of FeNi (31% Ni) and FeCo (49% Co) alloys (particle size 800, 500, 300, and 160 Å), for which the probability of the effect fell with decreasing particle size, and for SnO_2 with a particle size of about 60 Å, for which f was also smaller than in macroscopic SnO_2. The literature data[15-17,36,50] and also our latest measurements are given in the Table.

Mössbauer effects in different substances

Substance	References	Size, Å	T, °K	f'_{exp}	Method of preparation
β-Sn	15	250	80	0.25	aerosol
		250	300	0.022	
		foil	80	0.35	
		foil	300	0.06	
FeNi (31% Ni)		160	80	0.7 rel. units	aerosol
		160	300	0.5 rel. units	
		800	80	1.4 rel. units	
		800	300	1.1 rel. units	
FeCo (49% Co)		160	80	0.7	aerosol
		160	300	0.5 rel. units	
		800	80	1.4 rel. units	
		800	300	1.3 rel. units	
W	16	30	4	0.57	hydrolysis of tungsten hexacarbonate
		1 μm	4	0.61	
Au	50	60	25	0.16	hydrosol
		60	60	0.07	
		200	25	0.14	
		200	60	0.05	
SnO_2		60	80	0.45	aerosol
		60	300	0.11	
		powder	80	0.9	
		powder	300	0.6	
Fe_2O_3	17	20—30	300	0.31—0.43	hydrosol
			100	0.37—0.51	
Pt	37	100	4	2-8 rel. units	platinum in silica gel pores
		foil	4	2-8 rel. units	

It follows from the Table that in almost all cases, with the exception of gold and platinum, the probability of the effect falls with decrease of particle size. However, the absolute values of f may oscillate somewhat, depending on the method of preparation of the particles[17] and therefore it is desirable to perform experiments of this kind for particles of 3–4 different dimensions, prepared by the same method (the aerosol method is apparently preferable, since under these conditions more nearly spherical particles are obtained). The increase of f for individual tin-119 atoms on the surface of platinum compared with polyatomic tin particles on platinum[12] and also the constancy of f for platinum in the pores of silica gel compared with platinum foil[34] can be included among the effects related to the increase of f with decreasing particle size. The results obtained for tin on the surface of platinum may, however, be attributed to the diffusion of tin into the bulk of platinum.

The most probable explanation of the increase of f with decreasing particle size is that the effect of the "compacting" of the phonon spectrum (as a result of the long wavelength cut off) predominates over surface effects. Unfortunately the influence of the surface can diminish f in different ways, depending on the method of preparation of the specimen. This makes it difficult to assess quantitatively the decrease of f taking into account the increase caused by the "compacting" of the phonon spectrum. Nevertheless experiments show that for gold and platinum the effect of the low-frequency component of the phonon spectrum on f is more significant than for the other substances investigated. This makes it possible to characterise the contribution of the long-wavelength part of the spectrum to the overall phonon spectrum by investigating very small particles of the substance.

2. Magnetic Properties of Small Particles. Superparamagnetic Phenomena

Thermal fluctuations of magnetisation do not occur in massive specimens which remain magnetically ordered up to the Curie (T_C) and Néel (T_N) points. As a result, whenever $T < T_C$, T_N, magnetic fields are found at the nuclei and the specimen shows macroscopic magnetisation. However, as the dimensions of the specimens decrease, thermal fluctuations in the magnetisation of the entire particle begin to occur, which leads to an averaging of the macroscopic magnetisation to values characteristic of the paramagnetic state of matter and the disappearance of magnetic fields at the nuclei, although the substance is still in the magnetically ordered state. Such behaviour of matter in a highly dispersed state in fact characterises the phenomenon of superparamagnetism. Indeed, for finite volumes of the substance, the frequency of the fluctuations in magnetisation may be described by the formula

$$\nu = \nu_0 \exp\left(-\frac{Kv}{kT}\right),$$

where ν_0 is usually of the order of 10^{10} s^{-1}, K (erg cm^{-3}) is the constant of anisotropy characterising the energy necessary to "overturn" the magnetisation vector and v is the volume of the particle. With increase of temperature, the fluctuation frequency ν increases, and, depending on the method used to investigate small particles of this kind, the latter will exhibit at a given temperature the properties either of magnetically ordered or magnetically disordered substances. This leads to an effective lowering of the Curie and Néel points as the particle size is reduced. By superimposing an external magnetic field of several kilo-oersteds, it is possible to increase artificially the constant of anisotropy by an amount μH:

$$\nu = \nu_0 \exp[(-Kv + \mu Hv)/kT],$$

where μ is the magnetic moment of the atom and H the external magnetic field. This provides an additional equation for the determination of the unknown volume of the particles. Mössbauer spectroscopy is the only method available for the investigation of superparamagnetism, since, in contrast to usual procedures, it permits the investigation of the relaxation of magnetisation during a period of 10^{-8} s. The frequency of thermal fluctuations and the relaxation time of magnetisation τ are determined from the widening of the Mössbauer line[32]:

$$\tau = \frac{\hbar}{\Delta\Gamma}.$$

A second feature of small particles is the absence of phase transition points associated with the change in the direction of the magnetisation of the spin relative to the axis of the crystal field, for example the absence of the Morin point in haematite.

The first experiment on superparamagnetism by the γ-resonance method was performed by Nakamura et al.[51], who found that, for Fe_2O_3 particles 50 Å in diameter, the Néel point is markedly reduced compared with large particles and lies between 120° and 300°K ($T_N \simeq 1000$°K for the usual Fe_2O_3). At 120°K there is the usual six-line hyperfine structure characteristic of an antiferromagnetic material and at 300°K the spectrum consists of a doublet corresponding to the superparamagnetic state of Fe_2O_3. Subsequently similar experiments were performed to investigate the effective changes in the behaviour of the Curie and Néel points and to determine the constants of anisotropy. Two methods may be employed to determine the constants. Kündig et al.[27] suggested that the frequency of the precession of the nuclear spin in the magnetic field acting upon the nucleus be used as a characteristic for which the contribution by the hyperfine structure amounts to approximately 50% of the entire spectrum under conditions where the frequency of the thermal fluctuations of the magnetisation is equal to the frequency of the precession of the nuclear spin. By determining the average volume of the particles at a specified temperature or the temperature for a specified column, for which the above condition holds, and by substituting these values in the exponential equation, the constant of anisotropy is found. The volume of the particles is determined by some other procedure, for example from X-ray diffraction data.

It is possible to suggest another method, associated with the possibility of the determination of τ from Mössbauer spectra, as was done by Suzdalev et al.[32] or by Wickman et al.[52] In this case one observes the experimental relation between $\ln\tau = \ln\tau_0 - Kv/kT$ and $1/T$, from which it is possible to determine the values of $\ln\tau_0$ and Kv/k. Kündig et al.[27] investigated highly dispersed Fe_2O_3 with a particle size of about 100 Å prepared by impregnating silica gel with a solution of $FeCl_3$ and subsequent thermal decomposition to iron(III) oxide. They also observed a decrease of the Curie point below 300°K. By analysing the change in the spacings between the hyperfine lines, the authors showed that in such Fe_2O_3 particles there is no Morin transition in which the magnetisation becomes parallel to the crystal field gradient when the temperature is reduced. The constant of anisotropy for Fe_2O_3 is $K = 4 \times 10^4$ erg cm^{-3} according to experimental data.

Shinjo[53] and Van der Kraan and van Loef[54] investigated the highly dispersed state of the antiferromagnetic material hetite (α-FeOOH) with a particle size between 60 and 500 Å. Here $K = 1 \times 10^4$ erg cm^{-2} and therefore the lowering of the Néel point and the appearance of superparamagnetism are already appreciable for larger particles than in the case of Fe_2O_3. When the particle size is reduced, the anisotropy constant may diminish somewhat[27]. Ando et al.[55] investigated the antiferromagnetic material NiO by introducing cobalt-57 into this oxide. The Néel point for NiO is 523°K. For 100 Å particles, obtained by impregnating with a mixture of $Ni(NO_3)_3$ and cobalt-57 with subsequent heat treatment at 500°C in air, the Néel point fell to 200°K. The investigators were able to demonstrate, using the characteristics of the structure of the highly dispersed initial oxide (with an excess of oxygen relative to the stoichiometric composition), that the Fe^{2+} spectrum observed previously by Bhide and Shenoy[56] and Triftshäuser and Craig[57], disappears for small particles and only the Fe^{3+} spectrum remains, owing to the presence of oxygen in excess of stoichiometry.

Schuele et al.[58] investigated highly dispersed ferrites ($NiFe_2O_4$ and $CoFe_2O_4$) with a particle size between 100 and 200 Å. Since the anisotropy constant for cobalt compounds is higher, superparamagnetism appears for smaller particles than in the case of nickel.

Another branch of studies of this kind involves the determination of particle distribution with respect to dimensions by comparing two parts of a complex spectrum: (1) component corresponding at a given temperature to the non-magnetic state without a magnetic hyperfine structure which arises from small particles; (2) component corresponding to the magnetic state with a hyperfine structure which arises for larger particles.

A study of this kind was made by Gonser et al.[59] for particles of the $MgFe_2O_4$ ferrite deposited on MgO. The particle size varied both with temperature and with the duration of heat treatment of the $MgO-Fe^{3+}$ system in which the ferrite particles were deposited. The form of the spectra suggested that particles with a volume $v = 0.5 \times 10^{-18}$ cm^3 (deposition temperature 700°C, time 15 min), 1.4×10^{-18} cm^3 (800°C, 20 min), and 9.7×10^{-18} cm^3 (800°C, 90 min) were obtained, the relaxation times of the magnetisation being respectively $\tau = 0.18 \times 10^{-9}$, 0.31×10^{-9}, and 14×10^{-9} s. The authors used the following expressions for the calculation:

$$\tau = \frac{a}{\omega}\exp\left(\frac{|K_1|v}{12kT}\right), \quad \omega = \frac{4}{3}\gamma\frac{|K_1|}{M_s},$$

where $a \simeq 1$, γ is the gyromagnetic ratio, K_1 the constant of anisotropy along the light magnetisation axis, M_S the spontaneous magnetisation, and v the volume of the particle. Cobalt-57 particles were deposited in copper and investigated by the same procedure[60].

Assuming that the magnetic structure of the spectrum disappears when $\tau = 3 \times 10^{-9}$ s[52] and that $K = 2 \times 10^5$ erg cm^{-3} for the face-centred cobalt lattice, Masu et al.[60] found the critical volume of the particles at different temperatures. The average particle size was 100 Å and at 335°K a paramagnetic spectrum was already observed ($T_C \simeq 1000$°K for cobalt).

Lindquist et al.[61] investigated highly dispersed nickel with a small admixture of cobalt-57 obtained in silica gel pores. The particle size was about 30 Å. The relaxation time at 300°K was found to be $\tau = 2 \times 10^{-9}$ s by comparing with the calculations of Wickman et al.[52] the form of the hyperfine structure for the paramagnetic Fe^{3+} ions in the Ferrichrome A lattice. Lindquist et al.[61] observed that, when an external magnetic field is applied, the hyperfine structure of the spectrum of the paramagnetic component of the superparamagnetic material appears.

Gen et al.[62] studied the magnetic properties of the FeNi (13% Ni) alloy and found that in particles 100 and 500 Å in diameter a magnetic α-phase and a non-magnetic γ-phase are present, while macroscopic specimens contain only the α-phase. The α-phase is magnetically ordered for particles with diameters $<$ 100 and 500 Å. The study of the oxidation of such highly dispersed particles showed that, depending on the size, the relative proportions of the FeO, Fe_2O_3, and Fe_3O_4 phases change; the α-Fe_2O_3 and Fe_3O_4 phases are present in a highly dispersed state and have a reduced Néel point. The oxidation of the highly dispersed particles begins at 150°C, while that of macroscopic specimens takes place only at 500°C.

The study of the oxidation of highly dispersed systems permits the observation of the early stages in the oxidation,

as was shown in the oxidation of highly dispersed β-tin [13]. The lowering of the Curie point to 600°K for the highly dispersed FeCo alloy (49% Co) with a particle size of 160 Å was observed. These particles were obtained by the aerosol method, which probably yields the purest specimens for the investigation of the magnetic properties of particles, since the effect of another phase (metal, oxide, silica gel), which probably operated in all other investigations, is excluded. Despite the fact that for ferromagnetic materials superparamagnetism begins to have an effect for particle sizes of about 200 Å, the critical thickness of the film for which the hyperfine structure of the spectrum vanishes at a given temperature is much smaller. Lee et al.[28] investigated ultrathin iron films with a thickness of 1.2–15 Å deposited on a silicon support. The magnetic field had the usual value for 15 Å and thicker films but began to diminish as the thickness was reduced further. The results show that T_C and K vary sharply when the dimensions of the film become equal to twice the lattice constant.

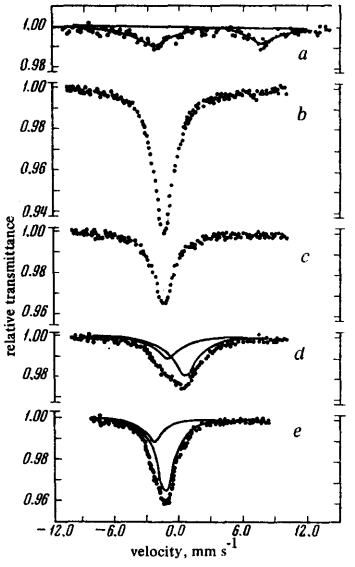


Figure 18. Spectra of gold-197 in the thermal decomposition of gold salts on η-Al_2O_3: *a*) $KAu(CN)_2$; *b*) and *c*) after high-temperature heat treatment; *d*) spectrum of $HAuCl_4$ after heat treatment at 140°K; *e*) spectrum after high-temperature heat treatment of $HAuCl_4$.

3. Topochemical Reactions

In the thermal or radiation-induced decomposition of a solid, the various phases interact and new substances are formed in a highly dispersed state and particles grow and become sintered. All these phenomena can be investigated very effectively by Mössbauer spectroscopy. Naturally, the results which we shall now discuss are directly related to the two fields dealt with previously, particularly to the preceding section. We shall divide topochemical reactions into two classes: (1) reactions in which the surface of the solid, which behaves as a carrier (for example silica gel or alumina), is involved and (2) reactions without a carrier.

Interesting studies of reactions of the first type were made by Delgass et al.[36] using the gold salts $KAu(CN)_2$ and $HAuCl_2$ on η-Al_2O_3 and MgO. The results of these investigations are presented in Fig. 18. The initial spectrum (*a*) of $KAu(CN)_2$ shows that, on drying at 140°C, the gold compound is not decomposed and spectra (*b*) and (*c*) demonstrate that, when the system is heat-treated in air, it is reduced to metallic gold. The spectra (*d*) for $HAuCl_4$ and η-Al_2O_3 at 140°C reveal the presence of metallic gold and a symmetrical gold complex and the spectrum (*e*) reveals, after heat treatment, yet another line, in addition to the line due to metallic gold.

An even more significant role of the carrier was noted in the studies of Hobson[42], Dunken et al.[63], and Arnold and Hobert[64]. Hobson[42] obtained iron(III) oxide by thermal decomposition of iron(III) nitrate and silica gel and alumina and the oxide was then reduced to hydrogen. He found that the distribution of Fe_2O_3 in η-Al_2O_3 with respect to particle size is wider than in the case of silica gel. Dunken et al.[63] observed that, after the thermal decomposition of $FeCl_3$ in alumina pores, only the superparamagnetic Fe_2O_3 phase is obtained when the percentage content of iron in alumina is varied from 0.125 to 9%, while Fe_2O_3 consisting of various phases (superparamagnetic and antiferromagnetic) was obtained in silica gel pores.

Among investigations of the second type, we may mention the studies on iron oxalates and hexacyanoferrates(III). Gallagher and Kurkijan[65] studied the thermal decomposition of the oxalates $Fe_2(C_2O_4)_3.5H_2O$, $Ba_3[Fe(C_2O_4)_3]_2.8H_2O$, and $Sr_3[Fe(C_2O_4)_3]_2.2H_2O$. With increase of temperature, divalent iron appears in all three compounds. The authors[65] found that at 300°C the highly dispersed Fe_2O_3 phase appears. Further increase of temperature leads to the appearance of the usual Fe_2O_3 phase. Heat treatment of strontium oxalate at 700°C and above resulted in the formation of an iron(IV) complex, while barium oxalate did not form such a complex.

Suzdalev and coworkers[66,67] investigated by Mössbauer spectroscopy and derivative plot analysis the thermal decomposition of iron(II) and iron(III) oxalates in an atmosphere of nitrogen. Fig. 19 shows differential plots and Mössbauer spectra for the decomposition of these oxalates. Iron(III) oxalate has three phase transitions at 200°, 280°, and 400°C, while iron(II) oxalate has only two: at 200° and 400°C. The first phase transition corresponds to the appearance of iron(II) oxalate with simultaneous dehydration. The third transition of iron(III) oxalate and the second transition of iron(II) oxalate correspond to the appearance of the Fe_3O_4 phase in the usual polycrystalline phase. The second phase transition in iron(III) oxalate corresponds to the formation of highly dispersed Fe_2O_4 with a particle size of about 100 Å.

The radiolysis of iron(III) oxalates[68] also indicates the formation of iron(II) oxalate. The spectrum of the latter does not alter on radiolysis. Probably the energy of the bond between iron and the lattice is higher in the divalent iron oxalate than in the trivalent iron salt. At a dose of 200 Mrad equilibrium is established between iron(II) and iron(III) oxalates. The growth of Fe_2O_3 particles in the second phase transition in the thermal decomposition of iron(III) oxalate was also investigated as a function of temperature as well as the kinetics of particle growth at a constant temperature[69].

The change in particle size was estimated from the change of the ratio of the area under the hyperfine structure to the area under the paramagnetic component corresponding to smaller particles. It was shown that, with increase of temperature from 240 to 280°C, the particle

size increases and the contribution by the hyperfine structure rises also.

The results of the kinetic experiments show that at 240°C there is a slight increase in the contribution by the hyperfine structure over a period of 2–3 h and then no further changes are observed.

Probably heat treatment of the test substance at the same temperature leads to the establishment of a quasi-equilibrium state, since equilibrium is established only as a result of the coalescence of smaller particles. At 240°C the growth of Fe_2O_3 particles begins, which, however, differ markedly in their dimensions and initially their system is not in equilibrium. In a study of the kinetics of particle growth, measurements were made of the relaxation times associated with the establishment of an average particle size. At higher temperatures equilibrium is established faster. As a result, the quasiequilibrium average particle size is related to a definite temperature and the actual particle size depends on the duration of the heat treatment.

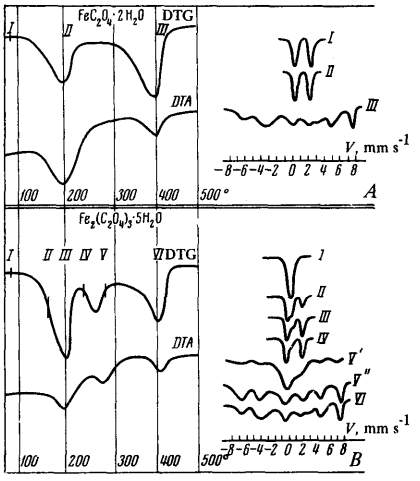


Figure 19. Differential plots (left-hand figure) and Mössbauer spectra (right-hand figure) obtained for the specimens at different temperatures: *A*) iron(II) oxalate; *B*) iron(III) oxalate.

The thermal decomposition of hexacyanoferrates was studied by Borshchagovskii et al.[70] using the compounds $LiY_8[Fe(CN)_6]_7.34H_2O$, $Sc_4[Fe(CN)_6]_3.xH_2O$, $Mn_2[Fe(CN)_6].6H_2O$, and $Sr_2[Fe(CN)_6].6H_2O$. All these compounds decompose by the same mechanism. At 160°C they are dehydrated and their spectra become somewhat wider, at 360°C iron atoms pass to the outer sphere, and at 760°C iron carbide (Fe_3C) is formed. By studying the kinetics, Borshchagovskii et al.[70] found that, after heat treatment for 2 h, metallic iron is formed from iron carbide.

In conclusion we shall consider the oxidation of highly dispersed tin (with particle sizes of 300 and 1000 Å).[14] It was shown that, up to the melting point of highly dispersed tin, its oxidation is hindered by the SnO_2 formed on the surface, but above the melting point the nature of the oxidation alters sharply. There is rapid formation of SnO, the proportion of which in material with a particle size of 300 Å becomes much greater than that of β-tin. However, up to 400 Å the spectra show the presence of unoxidised tin and for 1000 Å particles the amount of β-tin at an oxidation temperature of 300°C is greater than that of SnO.

These results show that up to 400°C the oxidation probably involves the reactions

$$2\,Sn + O_2 \rightarrow 2\,SnO,$$
$$2\,SnO \rightarrow SnO_2 + Sn,$$

and the reaction $2SnO + O_2 \rightarrow 2SnO_2$, a characteristic feature of which is the disappearance of SnO without the formation of β-tin, plays a very small role. About 400°C, this reaction begins to take place at a high rate and the entire tin is oxidised to SnO_2.

REFERENCES

1. V. I. Gol'danskii, "Primenenie Effekta Messbauera v Khimii" (Application of the Mössbauer Effect in Chemistry), Izd. Akad. Nauk SSSR, Moscow, 1963.
2. V. I. Gol'danskii, Uspekhi Fiz. Nauk, 89, 333 (1966).
3. M. Rich, Phys. Letters, 4, 153 (1963).
4. A. A. Maradudin and I. Meingailis, Phys. Rev., 133, A 1188 (1964).
5. L. S. Kothari, Phys. Letters, 24A, 382 (1967).
6. A. Corciovei and A. Berinde, Phys. Letters, 23, 32 (1966).
7. B. C. Clark, R. Herman, and R. F. Wallis, Phys. Rev., 139A, 860 (1965).
8. I. W. Burton and R. P. Godwin, Phys. Rev., 158, 218 (1967).
9. I. P. Suzdalev, "Primenenie Gamma-Rezonansnoi Spektroskopii k Issledovaniyu Fiziko-khimicheskikh Svoistv Poverkhnosti Tverdykh Tel, Sbornik MIFI" [Application of γ-Resonance Spectroscopy in the Study of the Physicochemical Properties of the Surface of Solids, MIFI (Significance of abbreviation obscure—Ed. of Translation)] Symposium, Atomizdat, Moscow, 1967.
10. R. F. Wallis, Surface Science, 2, 146 (1964).
11. F. G. Allen, Bull. Amer. Phys. Soc., 9, 296 (1964).
12. B. I. Bowles and T. E. Cranshaw, Phys. Letters, 17, 258 (1965).
13. E. R. Jones, I. T. McKinney, and M. B. Webb, Phys. Rev., 151, 476 (1966).
14. I. P. Suzdalev, E. F. Makarov, I. Ya. Garzanov, and L. A. Korytko, Kinetika i Kataliz, 6, 1108 (1965).
15. I. P. Suzdalev, M. Ya. Gen, V. I. Gol'danskii, and E. F. Makarov, Zhur. Exper. Teor. Fiz., 51, 118 (1966).
16. S. Roth and E. M. Hörl, Phys. Letters, 25A, 299 (1967).
17. I. S. Van-Wieringen, Phys. Letters, 26A, 370 (1968).
18. P. A. Flinn, S. L. Ruby, and W. L. Kehl, Science, 143, 1434 (1964).
19. I. P. Suzdalev, V. I. Gol'danskii, E. F. Makarov, A. S. Plachinda, and L. A. Korytko, Zhur. Exper. Teor. Fiz., 49, 1424 (1965).
20. I. P. Suzdalev, A. S. Plachinda, and E. F. Makarov, Zhur. Exper. Teor. Fiz., 54, 1556 (1968).
21. K. S. Singwi and A. Sjolander, Phys. Rev., 120, 1093 (1960).
22. V. I. Gol'danskii, I. P. Suzdalev, A. S. Plachinda, and L. G. Shtyrkov, Dokl. Akad. Nauk SSSR, 169, 872 (1966).
23. I. P. Suzdalev, A. S. Plachinda, E. F. Makarov, and V. A. Dolgopolov, Zhur. Fiz. Khim., 11, 2831 (1967) [Russ. J. Phys. Chem., No. 11 (1967)].
24. A. S. Plachinda, I. P. Suzdalev, V. I. Gol'danskii, and I. E. Neimark, Teor. Exper. Khim., 6, 347 (1970).

25. R. Barrer, R. F. Bartholomew, and L. V. C. Reis, J. Phys. Chem. Solids, 24, 51 (1963).
26. J. D. Donaldson and B. I. Senior, J. Chem. Soc., 12A, 1796 (1966).
27. W. Kündig, H. Bömmel, G. Constabaris, and R. M. Lindquist, Phys. Rev., 142, 327 (1966).
28. E. L. Lee, P. E. Boldue, and U. Violet, Phys. Rev. Letters, 13, 800 (1964).
29. S. I. Glass and M. Klein, Phys. Rev., 109, 288 (1958).
30. A. M. Afanas'ev and Yu. Kagan, Zhur. Exper. Teor. Fiz., 45, 1660 (1963).
31. G. K. Wertheim and I. R. Remeika, Phys. Letters, 10, 14 (1964).
32. I. P. Suzdalev, A. M. Afanas'ev, A. S. Plachinda, V. I. Gol'danskii, and E. F. Makarov, Zhur. Exper. Teor. Fiz., 55, 1752 (1968).
33. V. I. Gol'danskii, A. S. Plachinda, I. P. Suzdalev, and V. P. Korneev, Dokl. Akad. Nauk SSSR, 185, 141 (1969).
34. V. N. Baranovskii, G. M. Gorodinskii, L. M. Krizhanskii, V. I. Rogozev, and S. V. Tomilov, Radiokhimiya, 8, 369 (1966).
35. J. L. Mackey and R. L. Collins, J. Inorg. Nuclear Chem., 29, 655 (1967).
36. W. N. Delgass and M. Boudart, Catalysis Rev., 2, 129 (1968).
37. M. Blume, Phys. Rev. Letters, 14, 96 (1965).
38. M. M. Dubinin, Dokl. Akad. Nauk SSSR, 159, 166 (1964).
39. I. E. Neimark, Izv. Akad. Nauk SSSR, Ser. Khim., 969 (1965).
40. A. N. Karasev, L. S. Polak, E. B. Shlikhter, and V. S. Shpinel', Kinetika i Kataliz, 6, 710 (1965).
41. J. A. Morice and L. V. C. Rees, Trans. Faraday Soc., 64, 1388 (1968).
42. M. C. Hobson Jnr., Nature, 214, 79 (1967).
43. M. C. Hobson and H. M. Gager, "Fourth International Congress on Catalysis", Moscow, 1968, Report 48.
44. M. C. Hobson and A. D. Campbell, J. Catalysis, 8, 294 (1967).
45. A. N. Karasev, Yu. A. Kolbanovskii, L. S. Polak, and E. Sh. Shlikhter, Kinetika i Kataliz, 8, 232 (1967).
46. L. V. Skalina, I. P. Suzdalev, I. K. Kolchin, and L. Ya. Margolis, Kinetika i Kataliz, 10, 456 (1969).
47. I. P. Suzdalev, A. V. Shkarin, and G. M. Zhabrova, Kinetika i Kataliz, 10, 218 (1969).
48. K. Hauffe, "Elektronnye Yavleniya. Sbornik Kataliz" (Electronic Phenomena. Collected Papers on Catalysis) (Translated into Russian), Inostr. Lit., Moscow, 1958, p. 274.
49. Yu. V. Maksimov, I. P. Suzdalev, Yu. P. Yampol'skii, and K. P. Lavronskii, Dokl. Akad. Nauk SSSR, 183, 143 (1968).
50. S. W. Marshall and R. M. Wilenzik, Phys. Rev. Letters, 16, 219 (1966).
51. T. Nakamura, T. Shinjo, Y. Endon, N. Yamamoto, M. Shiba, and Y. Nakamura, Phys. Letters, 12, 178 (1964).
52. H. H. Wickman, M. P. Klein, and D. A. Shirley, Phys. Rev., 152, 345 (1966).
53. T. Shinjo, J. Phys. Soc. Japan, 21, 917 (1966).
54. A. M. Van der Kraan and I. I. van Loef, Phys. Letters, 20, 614 (1966).
55. K. I. Ando, W. Kündig, G. Constabaris, and R. M. Lindquist, J. Phys. Chem. Solids, 28, 2291 (1967).
56. V. G. Bhide and G. K. Shenoy, Phys. Rev., 147, 306 (1966).
57. W. Triftshäuser and P. P. Craig, Phys. Rev. Letters, 16, 1161 (1966).
58. W. I. Schuele, S. Shtrikman, and D. Treves, J. Appl. Phys., 36, 1010 (1965).
59. U. Gonser, H. Wiedersich, and R. W. Grant, J. Appl. Phys., 39, 1004 (1968).
60. S. Nasu, T. Shinjo, Y. Nakamura, and Y. Murakanii, J. Phys. Soc. Japan, 23, 664 (1967).
61. R. H. Lindquist, G. Constabaris, W. Kündig, and A. M. Portis, J. Appl. Phys., 39, 1001 (1968).
62. M. Ya. Gen, I. E. Eremina, V. A. Koltun, E. F. Makarov, V. A. Povitskii, and I. P. Suzdalev, Fiz. Tverd. Tela, 9, 3141 (1967).
63. H. Dunken, H. Hobert, and W. Meisel, Z. Chem., 6, 276 (1966).
64. D. Arnold and H. Hobert, Z. Chem., 8, 197 B (1968).
65. P. K. Gallagher and G. R. Kurkijan, Inorg. Chem., 5, 214 (1966).
66. I. P. Suzdalev, A. V. Shkarin, G. M. Zhabrova, V. I. Gol'danskii, L. A. Korytko, and B. M. Kadenatsi, Kinetika i Kataliz, 7, 919 (1966).
67. A. V. Shkarin, I. P. Suzdalev, G. M. Shabrova, and V. M. Kadenatsi, Teor. Exper. Khim., 3, 483 (1967).
68. A. V. Shkarin, I. P. Suzdalev, B. M. Kadenatsi, and G. M. Zhabrova, Khimiya Vysokikh Energii, 2, 77 (1968).
69. I. P. Suzdalev and Yu. F. Krutynskii, Kinetika i Kataliz, 10, 1255 (1969).
70. B. V. Borshchagovskii, V. I. Gol'danskii, G. B. Seifer, and R. A. Stukan, Zhur. Neorg. Khim., 12, 3291 (1967) [Russ. J. Inorg. Chem., No. 12 (1967)].

Institute of Chemical Physics,
USSR Academy of Sciences,
Moscow